

Complete identification of alkali sites in ion conducting lithium silicate glasses: a computer study

Heiko Lammert,^{*} Magnus Kunow,[†] and Andreas Heuer[‡]

*Institute of Physical Chemistry,
Schlossplatz 4/7, D-48149 Münster
and Sonderforschungsbereich 458*

(Dated: May 21, 2019)

Abstract

The available sites for ions in a typical disordered ionic conductor are determined. For this purpose we devised a straightforward algorithm which via cluster analysis identifies these sites from long time ionic trajectories below the glass transition. This is exemplified for a lithium silicate glass $(\text{Li}_2\text{O})_x(\text{SiO}_2)_{(1-x)}$ for $x = 0.5$ and $x = 0.1$. We find that the number of sites is only 3% for $x = 0.5$ and 8% for $x = 0.1$ larger than the number of ions. This result suggests that a theoretical description of the dynamics in terms of mobile vacancies is most appropriate. Furthermore identification of the ionic sites allows one to obtain detailed characteristics of the ionic motion, e.g. quantification of correlated forward-backward motion.

PACS numbers: 66.30.Hs, 61.43.Fs, 02.70.Ns

Ion conducting glasses have been investigated by various experimental methods, including EXAFS [1, 2], NMR [3, 4, 5], and conductivity spectroscopy [6, 7, 8]. Whereas quite detailed information about the local structure has become available the mechanism of dynamics is still under debate although consensus has been reached that ion dynamics can be described as jumps of the mobile ions [9, 10, 11]. Whereas some authors stress the relevance of the disordered energy landscape [10, 12] supplied by the network, others relate the complexity of ion dynamics to the Coulomb interaction among mobile ions [6]. Furthermore it has been argued from structural considerations that the distribution of alkali ions will be inhomogeneous [13].

For a closer understanding of ion dynamics microscopic information as supplied by molecular dynamics simulations is highly welcome. Jund et al. [14] found preferential pathways as a dynamical phenomenon by counting the number of different alkali ions that passed through subvolumes of the simulation box. The resulting subvolumes visited by the largest number of different alkali ions may be interpreted as fast areas. They form a network of conduction paths. Oviedo and Sanz have argued on a qualitative basis that for alkali concentrations lower than 10% the alkali ions are always surrounded by non-bridging oxygens (NBOs) despite the overall small number of NBOs [15]. This implies that new NBOs are formed via breaking of Si-O bonds along the alkali trajectory. In contrast, for higher concentrations hopping dynamics between so-called micro-channels is proposed such that no formation of new NBOs would be necessary. Thus one may hope that for alkali concentrations of 10% and higher well-defined alkali sites are present. Cormack [16] has recently investigated the mechanism of sodium migration in simulations of $(\text{Na}_2\text{O})_{0.25} \cdot (\text{SiO}_2)_{0.75}$ glasses, observing a few sequences of jumps between selected sites. He interpreted the resulting dynamics as the motion of vacancies and pointed out that the identification of *all* sites in the glass, empty or populated at a given time, would be most useful for obtaining a deeper understanding of the kinetic mechanisms. So far this identification is only possible for crystals like CaF_2 , where the available sites are known from the crystal structure [17].

Determination of all alkali sites in the silicate network is the purpose of this work. These sites can be interpreted as regions in the network where the potential energy for alkali ions is low and which are therefore sufficiently attractive for ions to stay there. Thus determination of the ionic sites is equivalent to determining the effective energy landscape experienced by the ions. The potential energy involves the network contribution as well as the averaged

interaction with other ions.

We analyse lithium silicate glasses $(\text{Li}_2\text{O})_x(\text{SiO}_2)_{(1-x)}$ with $x = 0.5$ and $x = 0.1$. The system size has been chosen such that for $x = 0.5$ we have 384 lithium ions and for $x = 0.1$ 80 lithium ions. Simulations are performed in the NVT ensemble at temperatures 640 K and 920 K and simulation box lengths 22.96 Å and 25.69 Å, respectively. The temperatures have been chosen such that the lithium diffusion constants are comparable (see below). The resulting densities match experimental values [18]. We use a BKS-type potential developed by J. Habasaki [19]. Previous studies with this potential have shown good agreement with experimental results for static and dynamic quantities [20, 21, 22]. The molecular dynamics simulations are performed with a modified version of Moldy [23]. Since both temperatures are below the respective glass transition temperatures we proceed in two steps. We start from a configuration which was first equilibrated just above the glass transition. It is then propagated at the selected temperature for ca. 20 ns in the NVT ensemble until the lithium subsystem is equilibrated. Afterwards we perform a production run for approximately 50 ns. During this run, positions of all particles are recorded every 0.1 ps. More details about the simulations can be found in [22]. We checked the validity of our results for independent data of up to 10 ns duration. This time is long enough for the lithium dynamics to become diffusive in our systems (see below), so that just the dynamics relevant for ionic transport is included.

Based on the lithium trajectories we have devised a straightforward algorithm to identify ionic sites. As a basic idea we let the ions decide via their dynamics where good sites are rather than determining the potential energy, as done e.g. in [24]. First the simulation box is divided into cubic cells with size approx. $(0.3 \text{ Å})^3$. They are small enough to enable resolution of the shape of the ionic sites. We count during our MD-run during how many time steps a cell is visited by a lithium ion. The cells with nonzero counts describe the portion of the system that has been visited by lithium ions. These cells include the lithium sites as well as the connecting paths between them. To identify the ionic sites and to eliminate the paths between the sites, cells with only a few counts are dismissed. The limiting value has been adjusted such that $A \approx 90\%$ of the total number of counts is contained in the selected cells. With these cells a cluster analysis is performed. Cells which share a face are grouped into one cluster. Cells that are not directly or indirectly connected over common faces form different clusters. Such clusters of frequently occupied cells may either contain a

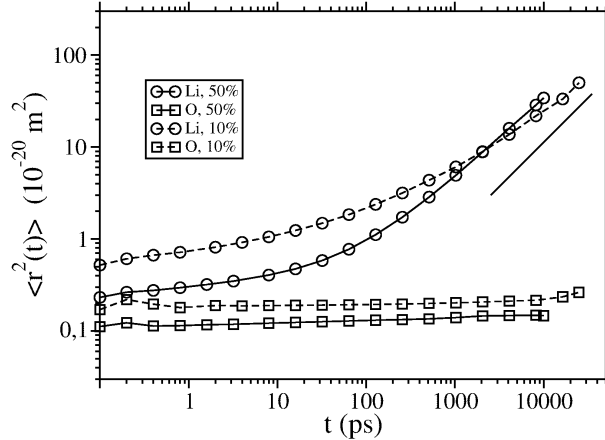


FIG. 1: Mean square displacements of lithium and oxygen in the simulations. Included is a line with slope 1.

single ionic site or sometimes also two or three ionic sites (see below). The value of A has been chosen by the condition that the number of distinct ionic clusters is a maximum. For a smaller threshold some lower populated clusters would not have been detected, for a larger threshold distinct clusters would be connected to single clusters because the transition path would be included. The precise value of A is of no relevance for the latter analysis.

In Fig. 1 we report the mean square displacement of oxygen and lithium. Evidently, the oxygen ions are localised on the ns-time scale. The network of silicon and oxygen atoms and with this the lithium sites can therefore be considered as static. As a consequence the ionic clusters are basically unmodified during the our run. Interestingly, as shown recently [25, 26] the remaining local fluctuations of the network are nevertheless essential in promoting the ionic jumps. In contrast, the dynamics of the lithium ions becomes diffusive for $t_{diff} \approx 1$ ns for $x = 0.5$ and $t_{diff} \approx 10$ ns for $x = 0.1$, as obtained from longer simulations.

For $x = 0.5$, 378 clusters are found, which contain 2.9% of the simulation volume. For $x = 0.1$, 76 clusters are found, containing 1.3% of the volume. The result is illustrated in Fig. 2, showing a snapshot of a slice through each system. The silicate network is shown as tubes, with silicon bright and oxygens dark. Lithium ions are depicted as large spheres. The white objects are the clusters obtained from the analysis described above, with each small white sphere representing one of the cells. It can be seen that the clusters are in fact discrete objects of compact shape. Most of the lithium ions reside inside of one of these clusters, and most of the clusters are occupied by exactly one lithium ion. As will be quantified further

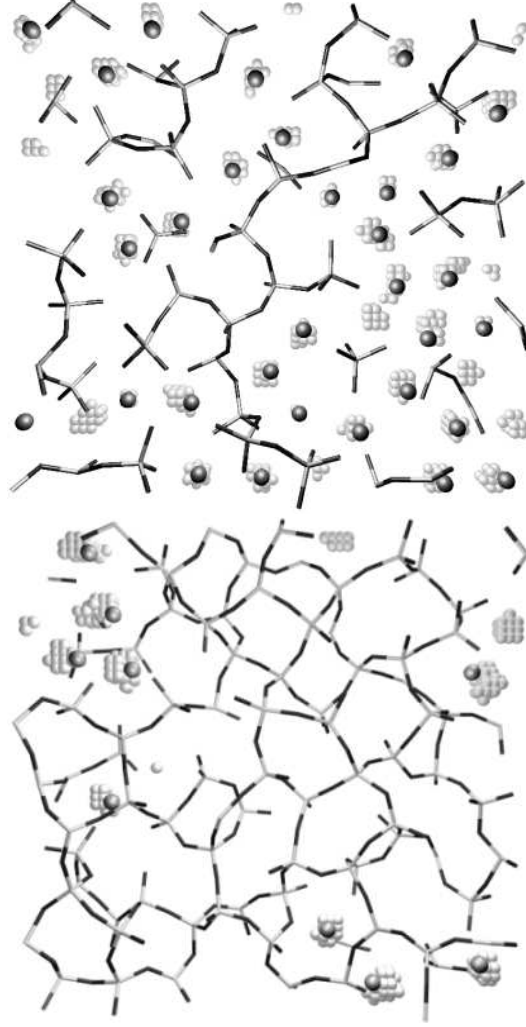


FIG. 2: Rendering of a slice of the simulation box for $x = 0.5$ (top) and $x = 0.1$ (bottom). (Created with vmd [27].)

below some clusters can accommodate up to three lithium ions.

On the basis of these clusters the dynamics of a lithium ion can be expressed as successive residences in clusters separated by shorter time intervals where the lithium ion is outside of any cluster. When a lithium ion leaves one cluster and moves into a different one, this sequence of events is recorded as a jump. In contrast, if an ion explores part of the volume outside a cluster without entering a second one and comes back to the original cluster, it is regarded as occupying the same cluster during the whole time. Consequently, the residence time of a lithium ion in a cluster is defined as the time between its jump into this cluster and the subsequent jump to another cluster. With this definition on average a lithium ion

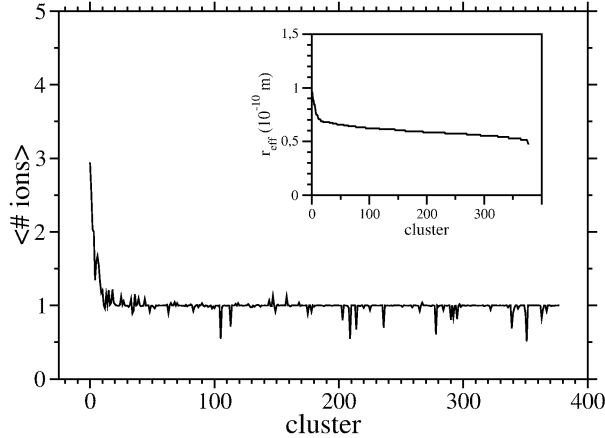


FIG. 3: Mean occupation of clusters. Inset: effective radius $r_{eff} \equiv (3V/4\pi)^{1/3}$ of clusters.

in the system with $x = 0.5$ belongs to a cluster at 99.5% of all times. The remaining 0.5% correspond to the time it takes to cross between different sites. For $x = 0.1$, the portion of times corresponding to jumps is 1.0%. The typical distance travelled by the lithium ions during a jump coincides well with the first maximum of the radial distribution function of the clusters in both cases. For $x = 0.5$, 93% of all jumps are inside the first neighbour shell (90% for $x = 0.1$) as defined by the first minimum of the radial distribution function. Thus the ion dynamics can be described as jumps between adjacent clusters. Long-range interstitial dynamics between distant clusters can thus be excluded.

Having defined the residence times the mean number of lithium ions occupying each cluster can easily be evaluated. It is plotted in Fig. 3 for $x = 0.5$, with the clusters ordered from left to right by decreasing volume V (the effective radius $r_{eff} \equiv (3V/4\pi)^{1/3}$ of the individual clusters is plotted in the inset). The occupation data confirms the impression gained from Fig. 2. For most clusters the value is close to unity. These clusters are occupied by a single ion during the largest part of the simulation. Their effective radius $r_{eff} \approx 0.6\text{\AA}$ is very similar. Only the largest clusters offer space for more than one lithium ion, i.e. they contain more than one site, and often they are indeed multiply occupied.

Generally an empty site must be available for a jump of a lithium ion. The total number of empty sites can be estimated from the occupation data in Fig. 3. For the larger clusters with cluster index < 19 we have taken the next higher integer number to estimate the number of available sites. In this way we find 3 clusters with 3 sites and 9 clusters with 2 sites. Starting from cluster index 14 one finds a few clusters with occupation number $1 + \epsilon$

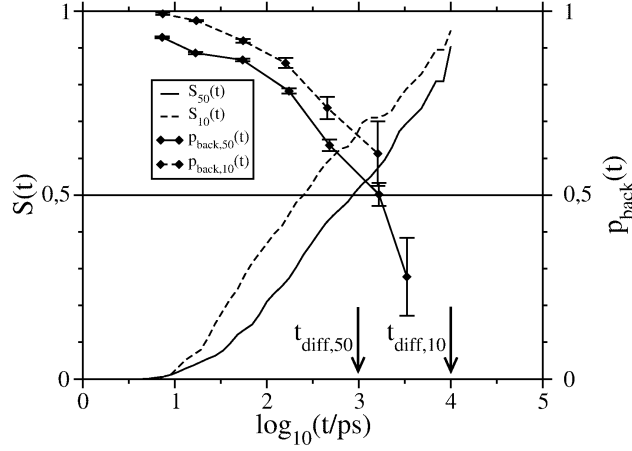


FIG. 4: Cumulative distribution function $S(t)$ of residence times and time dependence of the backjump probability $p_{\text{back}}(t)$ for systems with $x = 0.5$ and $x = 0.1$. Arrows mark the times at which the diffusive regime is reached, respectively.

with $\epsilon < 0.2$. Here it would be rather unphysical to attribute two sites to this cluster. Rather a more detailed analysis of explicit ion trajectories has revealed the following scenario. At most time instances a single ion stayed in this cluster. During the short times during which this ion explored the immediate neighborhood of this cluster without entering a new cluster (typical excursion length scales are 2 \AA from the center of the cluster) a second ion may briefly enter this cluster and immediately leave this cluster again. Thus one may either say that these clusters only contain a single site or, to be more conservative with respect to finding an upper bound of the total number of sites, attribute $1 + \epsilon$ sites to this cluster. With the latter variant we obtain 395 sites for our 384 lithium ions. Analogously, 86 sites were found for the 80 ions for $x = 0.1$. These results shed new light on the mechanism of ion dynamics. Rather than speaking of individual ions jumping between accessible sites it is more appropriate to speak to first approximation of vacancy dynamics, i.e. the dynamics of the non-interacting unoccupied sites in the energy landscape.

Actually, Dyre [28] has recently suggested this type of scenario based on general reasoning. He relates the possible near-equality of sites and ions to the effect that during network formation at the glass transition only a minimum number of sites will be formed due to energetic reasons. This scenario is also compatible with the counter-ion model, proposed by Dieterich and coworkers [29], but is at variance with single-particle approaches.

In the remaining part of this paper we would like to characterize the ionic dynamics in

terms of the individual clusters. Fig. 4 shows the cumulative distribution function $S(t)$ of residence times. Thus $S(t)$ denotes the fraction of clusters with an average residence time of less than t . Its median t_{median} , defined by $S(t_{median}) = 0.5$, is close to 1 ns for $x = 0.5$ and 250 ps for $x = 0.1$. These numbers have to be compared with the median of the transition time for a jump between two clusters, which is 500 fs for $x = 0.5$ and 200 fs for $x = 0.1$. This dramatic time scale separation clearly justifies the hopping picture in this kind of materials, as known from previous simulations [30]. The lithium dynamics on long time scales can thus be mapped on jumps between the clusters. Interestingly, it turns out for $x = 0.5$ that the residence time of ions in clusters with more than one site is significantly shorter (median of less than 100 ps) as compared to the average residence time. Thus the few large clusters are essential in promoting the ion dynamics in the alkali rich system. In contrast, for $x = 0.1$ the residence time does not depend on the cluster size.

For $x = 0.5$ and times less than $t_{diff,50} \approx 1$ ns (see Fig.1) only half of all lithium ions have performed a jump. The dispersive regime is thus dominated by the fast lithium ions. This would imply that forward backward motion is particularly present for the fast ions. To check this hypothesis we calculated the probability p_{back} that a jump from some cluster A to another cluster B is followed by a direct backjump to the original cluster A. We plot p_{back} against the residence time of cluster A, thereby averaging over clusters with similar residence time. The result is also shown in Fig. 4. One can clearly see that clusters with short residence times show a stronger tendency for a correlated forward-backward jump. For the fastest clusters, p_{back} reaches more than 0.9, which is several times higher than the statistical value which is close to the inverse of the number of nearest neighbor ions ($\approx 0.2 \dots 0.3$).

Finally, we would like to discuss a remarkable difference between both concentrations. Comparing the median t_{median} of the residence time distribution with t_{diff} one obtains $t_{median}/t_{diff} \ll 1$ for $x = 0.1$ and $t_{median}/t_{diff} \approx 1$ for $x = 0.5$. Partly this difference may be traced back to the higher probability of correlated backjumps. Whereas for $x = 0.5$ the backjump probability $p_{back}(t_{median}) \approx 0.55$ for $x = 0.5$ one has $p_{back}(t_{median}) \approx 0.8$ for $x = 0.1$. Naturally, the presence of backjumps strongly increases the time scale of t_{diff} .

Beyond the results shown in Fig. 4, a detailed analysis of the dynamics, i. e. in terms of cooperativity, becomes feasible. So far this was only possible for crystals [17]. Our approach may easily be generalised to more complex systems as mixed alkali systems and important

questions concerning, e.g., the character and the lifetime of the individual sites may be analysed.

We acknowledge interesting discussions with B. Doliwa, J. Dyre, M. Ingram, P. Jund, B. Roling, and M. Vogel and very helpful correspondence with J. Habasaki about this topic.

* hlammer@uni-muenster.de

† kunow@uni-muenster.de

‡ andheuer@uni-muenster.de

- [1] G. N. Greaves, S. J. Gurman, C. R. A. Catlow, A. V. Chadwick, S. Houde-Walter, C. Henderson, and B. Dobson, *Philos. Mag. A* **64**, 1059 (1991).
- [2] F. Rocca, *J. Phys. IV* **2**, 97 (1992).
- [3] H. Maekawa, T. Maekawa, K. Kawamura, and T. Yokokawa, *J. Non-Cryst. Solids* **127**, 53 (1991).
- [4] A. T. W. Yap, H. Förster, and S. R. Elliott, *Phys. Rev. Lett.* **75**, 3946 (1995).
- [5] B. Gee and H. Eckert, *J. Phys. Chem* **100**, 3705 (1996).
- [6] K. Funke, *Prog. Solid State Chem.* **22**, 111 (1990).
- [7] Y. Abe, H. Hosono, W. H. Lee, and T. Kasuga, *Phys. Rev. B* **48**, 15621 (1993).
- [8] F. Salam, J. C. Giuntini, S. S. Soulayman, and J. V. Zanchetta, *Applied Physics A-Materials Science & Processing* **60**, 309 (1995).
- [9] M. D. Ingram, *Phys. Chem. Glasses* **28**, 215 (1987).
- [10] S. D. Baranowskii and H. Cordes, *J. Chem. Phys.* **111**, 7546 (1999).
- [11] A. Bunde, M. D. Ingram, and P. Maass, *J. Non-Cryst. Solids* **172**, 1222 (1994).
- [12] J. C. Dyre and T. B. Schröder, *Rev. Mod. Phys.* **72**, 873 (2000).
- [13] G. N. Greaves, *J. Non-Cryst. Solids* **71**, 203 (1985).
- [14] P. Jund, W. Kob, and R. Jullien, *Phys. Rev. B* **64**, 134303 (2002).
- [15] J. Oviedo and J. F. Sanz, *Phys. Rev. B* **58**, 9047 (1998).
- [16] A. N. Cormack, J. Du, and T. R. Zeitler, *Phys. Chem. Chem. Phys.* **4**, 3193 (2002).
- [17] Y. Kaneko and A. Ueda, in *Molecular Dynamics Simulations*, edited by F. Yonezawa (Springer, 1992), no. 103 in Solid-State Sciences, pp. 249–256.
- [18] H. Doweidar, *J. Non-Cryst. Solids* **194**, 155 (1996).

- [19] J. Habasaki and I. Okada, *Molec. Simul.* **9**, 319 (1992).
- [20] J. Habasaki, I. Okada, and Y. Hiwatari, *J. Non-Cryst. Solids* **183**, 12 (1995).
- [21] R. D. Banhatti and A. Heuer, *Phys. Chem. Chem. Phys.* **3**, 5104 (2001).
- [22] A. Heuer, M. Kunow, M. Vogel, and R. D. Banhatti, *Phys. Chem. Chem. Phys.* **4**, 3185 (2002).
- [23] K. Refson, *Computer Physics Communications* **126**, 310 (2000).
- [24] J. Habasaki, I. Okada, and Y. Hiwatari, *J. Non-Cryst. Solids* **208**, 181 (1996).
- [25] E. Sunyer, P. Jund, and R. Jullien (2002), cond-mat 0212058.
- [26] C. A. Angell, L. Boehm, P. A. Cheeseman, and S. Tamaddon, *Solid State Ionics* **5**, 659 (1981).
- [27] W. Humphrey, A. Dalke, and K. Schulten, *J. Molec. Graphics* **14**, 33 (1996).
- [28] J. Dyre (2002), cond-mat 0207722.
- [29] W. Dieterich, D. Knödeler, and P. Penzig, *J. Non-Cryst. Solids* **172-174**, 1237 (1994).
- [30] J. Habasaki, I. Okada, and Y. Hiwatari, *Phys. Rev. B* **55**, 6309 (1997).